Mechanism for Anion and Sulfur-Radical Production by 1−18 eV Electron Impact on Dimethyl Disulfide Adsorbed on Ice

H. Abdoul-Carime and L. Sanche*

Group of the Canadian Institutes of Health Research in the Radiation Sciences, Faculté de Médecine, Université de Sherbrooke, Sherbrooke, Québec, Canada, J1H 5N4

Received: March 7, 2002; In Final Form: July 3, 2002

We report the 1−18 eV electron-stimulated desorption of the anions H^-, S^-, CH_3^-, and $(SCH_3)^-$ from dimethyl disulfide (CH_3SSCH_3) condensed on amorphous D_2O films physisorbed on Pt. Below 11 eV, the desorbed anions and their respective sulfur-radical counterparts $(CH_2SSCH_3)^•$, (CH_3SCH_3), $(SSCH_3)^•$, and $(SCH_3)^•$ are formed via dissociative electron attachment to CH_3SSCH_3 (i.e., from the formation and subsequent dissociation of temporary states of $CH_3SSCH_3^-$). At 4.5, 6.0, and 9.0 eV incident electron energies, different dissociative attachment channels compete for the production of these reactive species. Above 11 eV, the same anions are produced via dipolar dissociation with corresponding cation fragments. A negative species observed at 35 amu is attributed to the formation of long-lived or stable $(SHD)^-$ anions, produced via secondary reactions on the ice film. Anion desorption is shown to be enhanced by the presence of the water substrate.

Introduction

The interaction of high-energy particles with matter generates large quantities of secondary electrons with typical energies less than 20 eV.[1−4] For a given energy of the fast primary particle, the number and energy distribution of low-energy electrons depend essentially on the dielectric response function of the irradiated material.[5] Since this function does not vary appreciably according to the nature of the different molecules within biological cells,[6] secondary electrons of low energy have a fairly uniform spatial probability density distribution in irradiated biological media. Such electrons are involved in the fragmentation of biological and atmospheric molecules.[7−11] Dimethyl disulfide (CH_3SSCH_3, abbreviated as DMDS) is of interest to both atmospheric chemistry and radiobiology, since it is, on one hand, one of the most widespread sulfur pollutant; on the other hand, it provides a model system for the investigation of radiation damage to the disulfide bond, which is involved in the structure and stability of proteins.[12,13]

Recently, we have investigated the damage induced by low-energy electron impact to the DNA molecule,[9] as well as the corresponding mechanisms of dissociation of its constituent bases[14,15] and structural water.[16] However, in a cell, nucleic acid interacts very closely with proteins, for instance, via stacking interaction of their amino acid residues with the nucleic acid bases.[17,18] Therefore, fragmenting protein via low-energy electron attack may produce reactive radicals, which in turn can react with the nearby DNA. There is, thus, a need to investigate the action of slow electrons on proteins, more particularly at the molecular level, on vital components of protein basic constituents. DMDS can serve as a molecular model system for the study of the action of low-energy electrons on the disulfide bond found within proteins.[19]

Moreover, DMDS is also one of the most widely spread sulfur pollutants produced by both biogenic and anthropogenic sources.[20,21] Among the latter, we find petroleum chemistry, oil refinement, and other processes such as activation in the preliminary procedure of catalysis of various products (e.g., gasoline, diesel oil, kerosene) and intermediate solvation of pesticides, rubber, and lubricants.[20] Once emitted and transformed in the atmosphere, DMDS can play a significant role in the formation of tropospheric and stratospheric sulfate aerosols.[22,23] In particular, $CH_3S^•$ produced from DMDS reacts with ozone, water, and the $OH^•$ radical to form sulfur dioxide and sulfuric acid.[24,25] These compounds are known to contribute to rain acidity when falling down to Earth.[26]

Since both the DMDS moiety of proteins in cells and the DMDS molecule in the atmosphere are likely to be in contact with the water molecule, we have chosen to investigate the interaction of 1−18 eV electrons with DMDS condensed on amorphous ice films. Although the interaction of the disulfide bonds with water in cells is not necessarily well represented by DMDS layers adsorbed on low-temperature ice, our sample preparation should provide conditions closer to biology, than the metal or semiconductor substrates usually used in surface experiments. The impact of 1−18 eV electrons on DMDS on top of the water substrate produces H^-, S^-, SH^-, CH_3^-, $(SCH_3)^-$, and SHD^- anions. From the incident electron energy dependence of the yields of the anions H^-, S^-, CH_3^-, and $(SCH_3)^-$, we find that, below 11 eV, these species are produced via dissociative electron attachment (DEA); i.e., by the dissociation of intermediate anions $[H_3C−S−S−CH_3]^{*-}$ into one of these stable anions and one or more radicals (e.g., $(H_3CSS·CH_2)^•$, $(CH_3SCH_3)^•$, $(SSCH_3)^•$, and $(SCH_3)^•$).

Experimental Procedures

The electron-stimulated desorption (ESD) of anions from DMDS condensed on multilayer D_2O films is measured in a vacuum chamber held at a pressure of $\sim 10^{-10}$ Torr, reached by a 400 $L·s^{-1}$ ion pump.[12] Multilayer films are grown on a polycrystalline Pt foil, cleaned prior to each deposition by resistive heating at 1200 K, and maintained at 90 K with liquid nitrogen. Molecules are introduced in the chamber via a

* Correspondence should be addressed to this author at the Départemente de Médecine Nucléaire et Radiobiologie, Faculté de Médecine, Université de Sherbrooke, Sherbrooke, Québec, Canada, J1H 5N4. Tel: (819)-346-1110, ext 14907; FAX: (819)-564-5442; E-mail: lsanche@courrier.usherb.ca.

10.1021/jp0206525 CCC: $22.00
Published on Web 11/01/2002

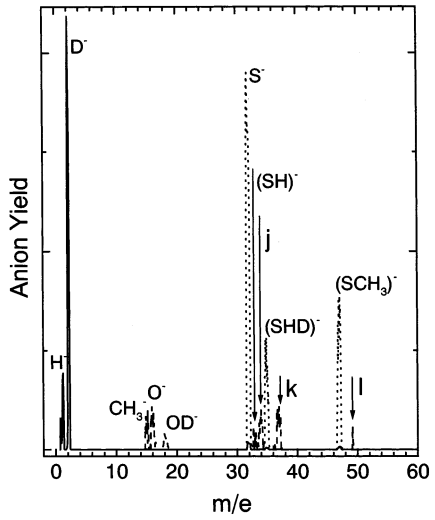

Figure 1. Masses of stable anions desorbing from a monolayer (ML) film of DMDS condensed on a 5-ML film of amorphous D_2O, physisorbed on Pt, and bombarded by a 100-nA beam of 9-eV electrons. The dotted curves have been multiplied by a factor of 50 and the dashed curves by a factor of 100. The peaks labeled "j, k, l" represent the isotopic ^{34}S-containing species. The $(SH)^-$ peak also includes a contribution from the $^{33}S^-$ anion (see text).

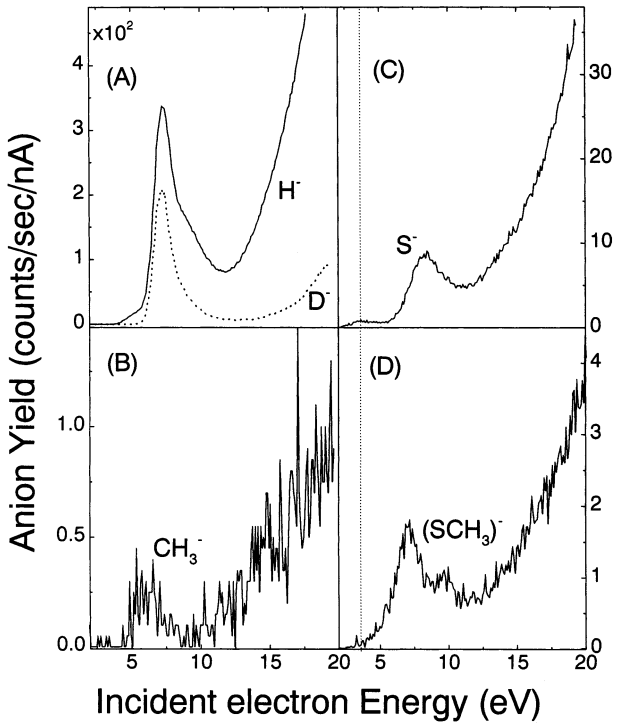

Figure 2. Incident electron energy dependence of (A) H^- (solid line) and D^- (dotted line), (B) CH_3^-, (C) S^-, and (D) $(SCH_3)^-$ ion yields desorbed under 80-nA electron bombardment of a monolayer of DMDS condensed on top of a 5-ML film of amorphous D_2O, physisorbed on Pt. The D^- signal (dotted curve in A) has been attenuated by a factor of 3.

stainless-steel tube connected to a gas-handling system. The film is bombarded at an incident angle of 70° from the surface normal, for approximately 60 s, by an 80−100 nA electron beam. The latter is produced by a commercial electron gun (Kimball Physics Inc.) with a resolution of 0.5 eV fwhm. The incident electron energy is calibrated by measuring the onset of the current transmitted through the film.[27] The film thickness is determined within 50% accuracy by correlating the condensation time to the saturation of the anion signal.[14,28] Desorbing anions are collected by an ion lens and detected by a mass spectrometer (Extrel 150-QC). Approximately one monolayer (ML) of CH_3SSCH_3 is deposited on top of 3−5 ML of D_2O. The role of the D_2O layer spacer is 2-fold: it prevents potential S−S bond cleavage and chemisorption on the Pt surface[29] and simulates the water cluster on which DMDS is bonded, either in high altitude atmosphere or within biological environment. Materials were purchased from Aldrich Ltd. (98% purity) and further purified by several freeze−thaw cycles prior to deposition.

Results and Discussion

Low-energy (1−18 eV) electron bombardment of DMDS/D_2O films produces not only D^- and H^- as the most intense negative fragments, but also the weaker anionic species CH_3^-, O^-, OD^-, S^-, $(SCH_3)^-$, and a 35 amu anion, as shown by the mass spectrum in Figure 1, recorded with a 9 eV incident electron beam. A priori, the 35-amu negative species can be attributed to the formation of stable or long-lived $(SHD)^-$ or the $(SH_3)^-$ anion, but the signal at 35 amu disappears in the absence of D_2O. We therefore ascribe this peak to the formation of $(SHD)^-$. The anionic fragments labeled "j, k, l" in Figure 1 are identified as the isotopic sulfur species $^{34}S^-$, $(^{34}SHD)^-$, and $(^{34}SCH_3)^-$, respectively, according to the natural abundance of ^{34}S relative to that of ^{32}S.[30] The weak signal at 33 amu is mainly attributed to the $(SH)^-$ anions, with a small contribution from $^{33}S^-$.

In our spectrometer, an anion with a mass of 35 amu would take about 10−100 μs to arrive at the detector depending on its initial kinetic energy. This time window sets a lower limit on the lifetime of $(SHD)^-$. The latter was suggested as an intermediate complex $(SH^-\!-\!D)$ in the formation of SD^- via charge transfer in reactive scattering S^-+D_2 experiments.[31−33] Its lifetime is however considered to be very short: of the order of the lifetime of the intermediate state SD_2^- (i.e., ∼10 fs) in the collision.[33] Although theoretical calculations on the $(SHH)^-$ ground-state potential energy surface have shown a deep well with a potential barrier,[34] stable $(SHH)^-$ has not been reported yet experimentally. The $(SHD)^-$ anion we detect here is probably in the ground-state configuration. In our measurements, the presence of deuterium indicates that $(SHD)^-$ most likely arises from the reaction of DMDS with D^- produced by DEA to D_2O. Since $(SHD)^-$ must have sufficient kinetic energy (∼1 eV) to escape the attractive polarization force at the film surface, it must arise from a dissociative intermediate state.[35] We therefore suggest that the following reactions lead to $(SHD)^-$ desorption within the femtosecond time scale, i.e.:

$$e^- + D_2O \rightarrow D_2O^- \rightarrow D^- + OD \quad (1)$$

$$D^- + CH_3SSCH_3 \rightarrow (CH_3SSCH_3D)^- \rightarrow (SHD)^- + CH_3SCH_2 \quad (2)$$

In other words, some $(CH_3SSCH_3D)^-$ intermediate species must exist and dissociate into $(SHD)^-$ and CH_3SCH_2 in order for $(SHD)^-$ to be propelled toward vacuum with sufficient initial kinetic energy to overcome the induced polarization potential (∼1 eV) which attracts the anion toward the surface.[7]

Figure 2 exhibits the ESD yields of D^-, H^-, CH_3^-, S^-, and $(SCH_3)^-$ as a function of electron energy. The energy of the peaks and shoulders present in these curves and the yield functions of $(SH)^-$ and $(SHD)^-$ (not shown) are given in Table 1. The line shape of such yield functions (i.e., pronounced

TABLE 1: Peak Positions (±0.5 eV) Observed in the Anion Yields Produced by Electron Impact on DMDS/D_2O Films Grown on a Platinum Substrate[a]

H^-	S^-	CH_3^-	SH^-	SCH_3^-	D^-	O^-	OD^-	SHD^-
	3.7		4.0	3.7*				
5*		5.8		6.1				5.5
7.4					7.2	7.8	7.3	
9.0	8.4		9.5	8.9				7.5
						12.8	12.1	

[a] An asterisk represents a shoulder or a faint peak.

maxima superimposed on an increasing monotonic background) can be generally attributed[7] to a contribution from the formation of dissociative transient anions, which produces the peaks, and another one from dipolar dissociation (DD). In the gas phase, the width of the peak arises from a convolution of the dissociation and resonance widths. The former represents the energy window accessible in the Franck−Condon region for electron attachment from the ground-state configuration to form the dissociative anion; the latter depends on the lifetime of the resonance. In ESD from condensed films, additional broadening mechanisms contribute to the peak width.[7] DD results from the dissociation of a neutral excited state into a positive and a negative ion, the latter being detected in the anion yield function.[7,11] Unless electron resonances (i.e., transient anions) decay in the DD channel,[14,35] the anion signal arising from DD does not exhibit any structure, since it is governed by direct (nonresonant) electronic excitation via inelastic scattering of the incoming electron. In this article, we focus our discussion on the lowest energy process (i.e., dissociative electron attachment, DEA).

The solid and dotted curves in Figure 2(A) represent H^- and D^- yields, respectively. The vertical gain of the D^- signal has been reduced by a factor of 3 in this figure. Below 10 eV incident electron energy, these anion yield functions present structures which are typical signatures of DEA to both DMDS and D_2O. The energies of each peak or shoulder are listed in Table 1. The deuterium anions are generated via reaction H shown in Figure 3. The resonance structure observed for D^- at 7.2 eV has been studied intensively in the gas[36,37] and condensed[16,38−40] phases; it has been attributed to the formation of the $^2B_1$ dissociating core-excited state of D_2O^- with contributions from the $^2A_1$ and $^2B_2$ states of D_2O^- in the higher-energy portion of the D^- yield function. In ESD experiments from D_2O films, the energies and ion yields of the resonances vary with the temperature and morphology of the D_2O film.[40] Below 60 K, the work function of the ice films changes with temperature, and the DEA resonances shift to higher energy. The D^- ESD yield generally increases with temperature, but it deviates from this trend at temperatures corresponding to structural phase transitions in ice. These results were attributed to thermally induced changes in the hydrogen bonding network, which changes the lifetimes of the predissociative states that lead to ESD and which also allows for the reorientation of surface molecules. Very small quantities of O^- and OD^- anions have recently been detected above 4 eV from electron-induced dissociation of amorphous D_2O films in high-sensitivity experiments.[41] These anions are also observed to desorb in the present investigation. Their formation in gas-phase experiments has been attributed to reactions F and G in Figure 3 with a possible contribution to the OH^- signal arising from the reaction of O^- and H^- with H_2O.[36,37]

The H^- yield function in Figure 2(A) exhibits a resonant structure close to that of the D_2O^- resonance (i.e., at 7.4 eV). This structure should arise from the fragmentation of DMDS,

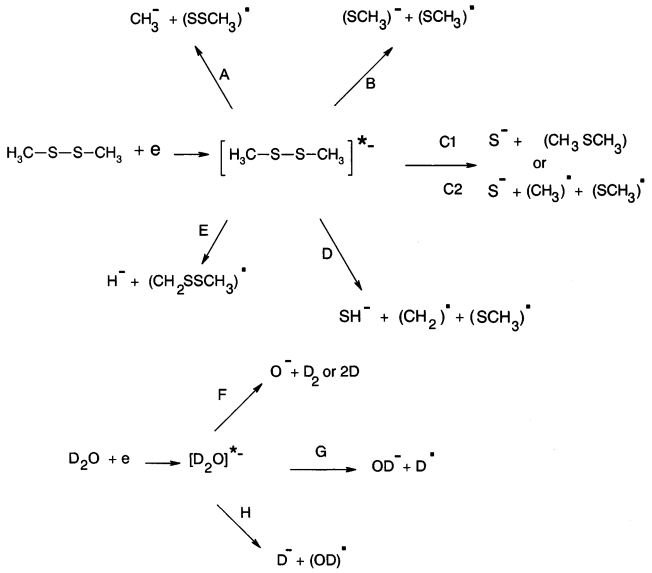

Figure 3. Possible dissociation pathways for negative ion production following low-energy electron attachment to condensed (A−E) DMDS and (F−H) D_2O. All negative anions represented were detected in the present experiment.

represented by reaction E in Figure 3, unless contamination by H_2O is present. The additional peaks observed at 4.5 eV (shoulder) and at 9.0 eV are definitively due to fragmentation of DMDS, since they do not appear in the anion yield function of D_2O.

The yield function of $(SHD)^-$ exhibits a peak at 7.5 eV, very close to the energy of the maximum in the D^- yield. This observation further supports D^- reactive scattering (i.e., reaction 2) as a possible mechanism responsible for $(SHD)^-$ desorption. The signal below 6 eV appears more difficult to explain by invoking a reaction with D^-, since very little D^- desorption occurs below that energy, as seen from the dashed curve in Figure 2(A). As shown from surface charging experiments,[42] this does not mean that D^- is not produced inside the film below 6 eV, but rather that only electrons of energy greater than 6 eV can produce D_2O^- with the nuclear arrangement on its potential energy surface necessary to provide D^- with sufficient kinetic energy to escape the induced polarization forces. Thus, reaction 2 could still occur in the film or at its surface below 6 eV. If the $(SHD)^-$ dissociation limit is sufficiently lower than that of D^- and/or due to the orientation of DMDS, $(SHD)^-$ is propelled in a vacuum with more kinetic energy perpendicular to the surface than D^-, desorption of $(SHD)^-$ should therefore be possible below 6 eV. In principle, $(SHD)^-$ desorption could also arise from reactive scattering of SH^- within the D_2O substrate. However, the probability of $(SHD)^-$ desorption via this reaction must be considered small, since the SH^- signal is found to be 5 times smaller than that of $(SHD)^-$ at 5.5 eV.

Low-energy electron impact experiments have also been performed with gaseous DMDS, where fragment anion production is observed only below 1 eV. Modeli et al.[43] observe a single peak in the yield functions of $(CH_2S)^-$, $(CH_3S)^-$, and $(CH_3SS)^-$. These results are in obvious contrast with the present ones, which indicate that anion desorption from DMDS condensed on ice films occurs only above 3 eV. Furthermore, we do not detect either $(CH_2S)^-$ or $(CH_3SS)^-$ anions, although $(CH_3S)^-$ fragments are seen in both phases. If the $(CH_2S)^-$ and $(CH_3SS)^-$ anions are formed within the 1−18 eV range in our films, the signal from those desorbing must lie below the detection limit. This does not mean that these negative fragments are not produced in the film, but that they could be undetectable

due to their insufficient kinetic energy to overcome the induced attractive potential.[44] However, the absence of detectable $(CH_2S)^-$ fragments, in the present experiment, indicates a lower probability to produce such anions than $(CH_3S)^-$ fragments by 1−18 eV electron impact on condensed DMDS, since the masses of the two fragments are similar (i.e., the escape probability from the surface is almost the same for both anions). In the gaseous DMDS experiments, the $(CH_3S)^-$ and $(CH_2S)^-$ signals only differ by a factor of about 3, but in this phase, the intermediate anionic state configuration is probably different, since it lies below 1 eV (i.e., at much lower energy). The large differences in anion signal between the two phases may not only be due to inhibition of anion desorption at low energies, but also reflect significant changes in the DEA process itself upon condensation of DMDS on ice. It is known that the parameters of DEA can be strongly altered by the presence of neighboring molecules: e.g., modification of the lifetime, energy and dissociation dynamics of the transitory molecular anion[7,44,45] and promotion and/or enhancement of a new dissociation channel.[7,46] We also note that gas-phase measurements[36,37] could discriminate *against* energetic ions, particularly if they emerge forward or backward with respect to the incident electron beam. Fast ions may then be more difficult to observe in gas-phase experiments; conversely, many of the low-energy ions detected in the gas phase do not desorb in the present experiment.

The yield function of the higher mass anions shown in Figure 2(B−D) exhibits resonant structures indicative of reactions A−D in Figure 3. DEA to DMDS induces sulfur−sulfur bond cleavage, as shown by the production of the $(SCH_3)^-$ anion. According to the energy calculation based on the value of DMDS's S−S bond energy of 3.2 eV[47] and on that of the electron affinity of the SCH_3 radical of 1.88 eV,[48] the threshold for $(SCH_3)^-$ formation is estimated to be 1.4 eV. This value can be compared with the experimental threshold of 2.0 eV found in the present measurements [Figure 3(D)]. The production of S^- anion may occur via reactions C1 and C2 (Figure 3), which require external energy transfer of ∼1.3 and ∼4.2 eV, respectively, according to the average C−S bond energy of 7.2 eV[30] and the sulfur electron affinity of 2.1 eV.[48] Within the lifetime of the transient anion $(CH_3SSCH_3)^-$, either exocyclic C−S ring cleavage or rearrangement of the nuclei occurs; i.e., concerted reactions[49,50] in which dissociation does not involve a single nuclear coordinate. These reactions lead to the formation of methyl, sulfur-contained anions and their neutral counterparts (reactions A−D in Figure 3). The observation of SH^- anions supports in part the concerted reaction mechanism, since hydrogen atoms are separated from the sulfur atoms in the molecule. The observation of a threshold for the production of S^- at 2.1 eV incident electron energy corroborates the concerted reaction mechanism (i.e., via reaction C1 in Figure 3) leading to the formation of the neutral dimethyl sulfide, $(CH_3)_2S$, counterpart at low incident electron energies. The extraction of S^- anion requires concomitantly bond cleavage and bond formation.

The structures observed near 6 eV (Table 1) in both $(CH_3)^-$ and $(SCH_3)^-$ yield functions in Figure 2 suggest competitive channels for anion dissociation: the excess free electron can be resonantly trapped by DMDS to create a transitory anion that dissociates along the intermolecular coordinate, e.g., $(SCH_3)^-$-(SCH_3), of a repulsive $(CH_3SSCH_3)^{*-}$ potential surface, up to a crossing point, where the other dissociative channel becomes available. Competitive fragmentation also probably occurs at approximately 4.5 and 9.0 eV for the production of H^-, SH^-, and $(SCH_3)^-$.

Near and above the first electronic excited state of molecules, the formation of *dissociative* transient negative ions usually occurs[7] via core-excited resonances (i.e., the formation of two-electron one-hole transitory anions). In this resonant process, the incoming electron transferring energy to electronically excite a molecule becomes captured by the electron−molecule potential of the excited state. Hence, the maxima in Figure 2 probably arise from the formation of such transient states. Furthermore, typically 4 eV below that of the corresponding positive ion, a predissociated core-excited resonance can form with two electrons in the Rydberg excited state bound to the positive ion core of the target molecule.[51] The ionization potentials of DMDS[52] lie at 9.2 and 13.4 eV for lone pair n_S and σ_{CS} excitation, respectively. The peaks near 6 eV in the yield functions of SCH_3^- and CH_3^- and those near 9 eV in the yield functions of H^- and SCH_3^- could therefore arise from such states.

Finally, we note that the contribution from nonresonant DD in the curves of Figure 2 could be represented by changing in Figure 3 the intermediate transient anion by electronically excited DMDS. In this case, CH_3SSCH_3* dissociates into the fragments shown in Figure 3 with a positive charge added on the (or one of the) neutral fragment(s) in each equation.

The effect of amorphous ice on the production of anionic fragments induced by both DEA and DD may be evaluated by energy-averaging between 1 and 18 eV the anion yield function of each negative fragment. Here, we compare the values obtained for S^-, SCH_3^-, and CH_3^- desorption with those obtained from ESD from physisorbed films of pure DMDS of the same thickness.[19] It has been measured, with the same apparatus and under the same experimental conditions, that (120, 16, and 4) × 10^{-10}, S^-, SCH_3^-, and CH_3^- ions/incident electrons, respectively, are desorbed from fragmentation of DMDS on an icy water substrate, whereas (330, 110, and 5) × 10^{-11} S^-, SCH_3^-, and CH_3^- ions/incident electron, respectively, are produced from dissociation of pure films of DMDS.[19] These results indicate that the presence of water enhances the desorption and probably the production of these anions. Moreover, the desorption of S^- and SCH_3^- via the S−S bond cleavage represents approximately 85% and 11% of the total desorbed "heavy" anion yields, respectively. These values can be compared to 70% and 22% of S^- and $(SCH_3)^-$ anions desorbed from the fragmentation of pure films of DMDS.[19] If S^- production operates via reaction C2, two highly reactive radicals, $(CH_3)^{\bullet}$ and $(SCH_3)^{\bullet}$, are produced.

Anion desorption via DEA from molecules physisorbed on amorphous ice has been investigated in the case of O_2 and hydrocarbons.[45,53,54] In most cases, the yields are found to decrease up to about an order of magnitude, in comparison to the yields emanating from films containing only the adsorbate molecules. Modification of the magnitude of the DEA process on ice has been attributed to interaction of the excited molecular orbitals of the transient anion with those of the H_2O molecule and the hydrogen-bonded network.[45,53,54] The interaction changes the lifetime of the transient anion. Since the probability for the transient species to dissociate before autoionization depends exponentially on this lifetime, molecular orbital perturbation by the ice surface may have considerable effect on anion desorption yields. The increase in the yields of the anions S^-, SCH_3^-, and CH_3^-, found in the present experiment, suggests that orbital interaction between amorphous ice and DMDS increases the lifetime of $(SCH_3)_2^-$.

Conclusion

We observed the electron-stimulated desorption of the anions H^-, S^-, SH^-, CH_3^-, $(SCH_3)^-$, and $(SHD)^-$ from dimethyl disulfide molecules physisorbed on amorphous ice films. From comparisons with the results obtained from films made of pure DMDS,[19] the presence of water molecules is found to enhance significantly the yield of the anions S^-, CH_3^-, and $(SCH_3)^-$. The 1−18 eV yield functions of H^-, S^-, CH_3^-, and $(SCH_3)^-$ indicate that below 11 eV, low-energy electrons fragment dimethyl disulfide via competitive DEA-induced dissociation pathways. Detection of these negative ions strongly implies the formation of the neutral radical counterparts $(SCH_3)^\bullet$, $(CH_2SSCH_3)^\bullet$, and $(SSCH_3)^\bullet$ and possibly that of $CH_3^\bullet$ and $CH_2^\bullet$ via reactions A−E in Figure 3. These radicals and the observed anions could therefore be generated by secondary electrons of low energy produced when ionizing radiation is incident on proteins, in which the disulfide bridge is an important covalent linkage between amino acids and/or chains of amino acids. When generated within chromosomes,[17,18] these radical species could react with the nearby DNA constituents and damage nucleic acid.

The radicals $(SCH_3)^\bullet$, $(CH_3)^\bullet$, $(CH_2)^\bullet$, $(CH_2SSCH_3)^\bullet$, and $(SSCH_3)^\bullet$ can also result from interaction of low-energy electrons generated by cosmic radiation[2] or radioactive waste, especially within solid materials, where the ionization rate is about 4 orders of magnitude higher than in the air due to the much larger molecular density. More particularly during cloud formation,[55] pollutants such as DMDS may become embedded or trapped for long times into H_2O aggregates.[56] Even at temperatures above the pollutant desorption temperature, diffusion may allow sufficient time for significant interaction with secondary electrons. Interestingly, some of the radicals formed by slow electrons are known to be the precursors of sulfur dioxide, as well as sulfuric acid, when oxidized in the atmosphere.[23−26] If the dominant "heavy ion" product S^- proceeds via reaction C2 in Figure 3, $(CH_3)^\bullet$ and $(SCH_3)^\bullet$ could react in the atmosphere with water and/or ozone to form SO_2 and/or H_2SO_4.[25,57] Moreover, the observation of CH_3^- via reaction A (Figure 3) shows clear evidence of production of the $(SSCH_3)^\bullet$ radical from fragmentation of DMDS induced by electrons. Although this radical has been only observed from secondary chemical reactions (e.g., reaction of CH_3S with S adsorbed on experimental reactor walls),[25] it has been shown to be as reactive as $CH_3S^\bullet$ with ozone.[25] The present information could therefore contribute to the evaluation of the impact of sulfur-compound emission on environmental modification.

Acknowledgment. This study was supported by the Canadian Institutes of Health Research (CIHR).

References and Notes

(1) ICRU Report Vol. 31, International Commission on Radiation Units and Measurements, Washington, DC, 1979.
(2) Cole, R. K., Jr.; Pierce, E. T. *J. Geophys. Res*. **1965**, *70*, 2735−2740.
(3) Pimblott, S. M.; Mozumder, A. *J. Phys. Chem.* **1991**, *95*, 7291−7300.
(4) Cobut, V.; Frongillot, Y.; Patau, J.-P.; Goulet, T.; Fraser, M.-J.; Jay-Gerin, J. P. *Radiat. Phys. Chem*. **1998**, *51*, 229−243.
(5) Inokuti, M. *Radiat. Eff. Defects Solids* **1991**, *117*, 143−162.
(6) LaVerne, J. A.; Pimblott, S. M. *Radiat. Res*. **1995**, *141*, 208−215.
(7) Sanche, L. *Scanning Microsc.* **1995**, *9*, 619−656.
(8) Lu, Q.-B.; Madey, T. E. *Phys. Rev. Lett*. **1999**, *82*, 4122−4125.
(9) Boudaïffa, B.; Cloutier, P.; Hunting, D.; Huels, M. A.; Sanche, L. *Science* **2000**, *287*, 1658−1660.
(10) Lacombe, S.; Cemic, F.; Jacobi, K.; Hedhili, M. N.; Lecoat, Y.; Azria, R.; Tronc, M. *Phys. Rev. Lett.* **1997**, *79*, 1146−1149.
(11) Lezius, M.; Parenteau, L.; Bass, A. D.; Sanche, L. *J. Phys. B* **1997**, *30*, 3527−3536.
(12) Wedemeyer, W. J.; Welker, E.; Narayan, M.; Scheraga, H. A. *Biochemistry* **2000**, *39*, 4207−4216.
(13) Carnovale, E.; Carbonaro, M.; Cappelloni, M.; Sabbadini, S. *J. Agric. Food Chem*. **1997**, *45*, 95−100.
(14) Abdoul-Carime, H.; Cloutier, P.; Sanche, L. *Radiat. Res.* **2001**, *155*, 625−633.
(15) Antic, D.; Parenteau, L.; Lepage, M.; Sanche, L. *J. Phys. Chem.* **1999**, *103*, 6611−6619.
(16) Simpson, W. C.; Orlando, T. M.; Parenteau, L.; Nagesha, K.; Sanche, L. *J. Chem. Phys*. **1998**, *108*, 5027−5034.
(17) Werner, M. H.; Clore, G. M.; Fisher, C. L.; Fischer, R. J.; Trinh, L.; Shiloach, J.; Gronenborn, A. M. *Cell* **1995**, *83*, 761−771.
(18) Suzuki, M. *Nature* **1990**, *344*, 562−565.
(19) Abdoul-Carime, H.; Cecchini, S.; Sanche, L. *Radiat. Res.* **2002**, *158*, 23−31.
(20) Turek, A.; Skrzydlinska, M.; Ptaszynski, B. *Collect. Czech. Chem. Commun*. **1996**, *61*, 1738−1744.
(21) Galloway, J. N.; Whelpdale, D. M. *Atmos. Environ*. **1980**, *14*, 409−417.
(22) Johnson, J. E.; Bates, T. S. *J. Geophys. Res*. **1993**, *98*, 23411−23421.
(23) Kley, D.; Crutzen, P. J.; Smit, H. G. J.; Vomel, H.; Oltmans, S. J.; Grassl, H.; Ramanathan, V. *Science* **1996**, *274*, 230−233.
(24) Turnispeed, A. A.; Barone, S. B.; Ravishankara, A. R. *J. Phys. Chem*. **1992**, *96*, 7502−7505.
(25) Domine, F.; Ravishankara, A. R.; Howard, C. J. *J. Phys. Chem*. **1992**, *96*, 2171−2178.
(26) Likens, G. E.; Weathers, K. C.; Butler, T. J.; Buso, D. C. *Science* **1998**, *282*, 1991−1992.
(27) Sanche, L. *J. Chem. Phys.* **1979**, *71*, 4860−4882.
(28) Rowntree, P.; Parenteau, L.; Sanche, L. *J. Phys. Chem.* **1991**, *95*, 4902−4909.
(29) Rufael, T. S.; Huntley, D. R.; Mullins, D. R.; Gland, J. L. *J. Phys. Chem*. **1998**, *102*, 3431−3440.
(30) *Handook of Chemistry Physics*, 73th ed; Lide, D. R., Ed.; CRC Press: Boca Raton, FL,1992−1993.
(31) Rempala, K.; Ervin, K. M. *J. Chem. Phys*. **2000**, *112*, 4579−4590.
(32) Fehsenfeld, F. C. In *Interaction between ions and molecules*; Ausloos, P., Ed.; Plenum: New York, 1974; p 387.
(33) Brenot, J. C.; Durupferguson, M.; Fayeton, J. A.; Goudjil, K.; Barat, M. *Chem. Phys.* **1994**, *179*, 557−571.
(34) Gritli, H.; Chambaud, G.; Rosmus, P. *Z. Naturforsch. A* **1996**, *51*, 151−154.
(35) Sanche, L.; Parenteau, L. *J. Chem. Phys*. **1990**, *93*, 7476−7482.
(36) Melton, C. E. *J. Chem. Phys.* **1972**, *57*, 4218−4225.
(37) Jurngen, M.; Vogt, J.; Staemmler, V. *Chem. Phys.* **1979**, *37*, 49−55.
(38) Rowntree, P.; Parenteau, L.; Sanche, L. *J. Chem. Phys*. **1991**, *94*, 8570−8576.
(39) Tronc, M.; Azria, R.; Le Coat, Y.; Illenberger, E. *J. Phys. Chem*. **1996**, *100*, 14745−14750.
(40) Simpson, W. C.; Sieger, M. T.; Orlando, T. M.; Parenteau, L.; Nagesha, K.; Sanche, L. *J. Chem. Phys.* **1997**, *107*, 8668−8677.
(41) Abdoul-Carime, H.; Bass, A. D.; Sanche, L., unpublished results.
(42) Sanche, L.; Deschênes, M. *Phys. Rev. Lett.* **1988**, *61*, 2096−2098.
(43) Modelli, A.; Jones, D.; DiStefano, G.; Tronc, M. *Chem. Phys. Lett*. **1991**, *181*, 361−371.
(44) Sambe, H.; Ramaker, D. E.; Parenteau, L.; Sanche, L. *Phys. Rev. Lett.* **1987**, *59*, 236−239.
(45) Huels, M. A.; Parenteau, L.; Sanche, L. *J. Chem. Phys*. **1994**, *100*, 3940−3956.
(46) Sanche, L. *Surf. Sci*. **2000**, *451*, 82−90.
(47) Lacombe, S.; Loudet, M.; Dargelos, A.; Robert-Banchereau, E. *J. Org. Chem.* **1998**, *63*, 2281−2291.
(48) Janousek, B. K.; Brauman, J. I. In *Gas-Phase Ion Chemistry*; Bowers, M. T., Ed.; Academic Press Inc.: New York, 1979; Vol. 2.
(49) Jacobsen, S.; Jensen, H.; Pedersen, S. U.; Daasbjerg, K. *J. Phys. Chem.* **1999**, *103*, 4141−4143.
(50) Stepanovic, M.; Pariat, Y.; Allan, M. *J. Chem. Phys*. **1999**, *110*, 11376−11382.
(51) Sanche, L.; Schulz, G. J. *Phys. Rev. A* **1972**, *6*, 69−86.
(52) Kishimoto, N.; Yokoi, R.; Yamakado, H.; Ohno, K. *J. Phys. Chem. A* **1997**, *101*, 3284−3292.
(53) Bass, A. D.; Parenteau, L.; Weik, F.; Sanche, L. *J. Chem. Phys*. **2001**, *115*, 4811−4818.
(54) Mozejko, P.; Parenteau, L.; Bass, A. D.; Sanche, L., unpublished results.
(55) Brasseur, G. P.; Orlando, J. J.; Tyndall, G. S. In *Atmospheric Chemistry and Global Change*; Oxford University Press: New York, 1999.
(56) Girardet, C.; Toubin, C. *Surf. Sci. Rep*. **2001**, *44*, 163−238.
(57) Seinfeld, J. In *Atmospheric Chemistry and Physics of Air Pollution*; John Wiley and Sons: New York, 1986.